

The Effects of Graft Geometry on the Patency of a Systemic-to-Pulmonary Shunt: A Computational Fluid Dynamics Study

*Jacek Waniewski, †Weronika Kurowska, ‡Jeremi K. Mizerski, *Anna Trykozko,
*Krzysztof Nowiński, §Grażyna Brzezińska-Rajszyś, and §Andrzej Kościeszka

**Interdisciplinary Center for Mathematical and Computational Modelling, Warsaw University, †Institute of Aeronautics and Applied Mechanics, Warsaw University of Technology, ‡Institute of Cardiology, and §The Children's Memorial Health Institute, Warsaw, Poland*

Abstract: The modified Blalock–Taussig shunt is a palliative operation for some congenital heart diseases. An artificial conduit with antithrombotic surface placed between the subclavian (or innominate) and the pulmonary artery supplies blood to the lungs in defects with decreased pulmonary flow. Clotting of the graft is the main cause of its failure. Stenosis of the arteries is also observed. The objective of the present study was to investigate the flow pattern in the graft to investigate the possibility that clotting is initiated by the stimulation of platelets by high shear stress, and the possible effect of the pathological wall shear stress on the stenosis formation. The model included the left subclavian artery (LSA), the left pulmonary artery (LPA), and the graft. The three-dimensional relative position and size of the arteries was obtained from a CT scan of real anatomy. Four different types of the graft with two different diameters (3 and 4 mm) and two different shapes (straight and curved) of the pipe, and one variable diameter pipe were inserted in the model. A pulsatile flow of 0.81 L/min on average was assumed at the inlet to LSA,

and 80% of the flow was directed through the graft. Computer simulations demonstrated a complex flow pattern with eddies and low velocity regions in the arteries at the anastomoses with the graft in all five models. An eddy was also found inside the straight 4 mm graft. A high pathological shear rate was present within the graft, with higher values in the 3 mm grafts. The fractional volume with a high (>2500 L/s) shear rate was between 2.5% and 4.5%, and that with a very high (>7500 L/s) shear rate between 0 and 1.5% of the model volume, and depended on the graft geometry and the phase of the cardiac cycle. Pathologically high (>3.5 Pa) and pathologically low (<1.0 Pa) wall shear stress, which may induce neointimal growth, was found in LSA and LPA. We conclude that the activation of platelets by high shear rate is possible within the graft, followed by their subsequent aggregation in the eddies with a low flow rate. Flow-induced changes of the vessel wall thickness (stenosis) can also appear, especially in the pulmonary artery. **Key Words:** Congenital heart disease—Hemodynamics—Blalock–Taussig shunt—Thrombosis—Stenosis.

The modified Blalock–Taussig (mB–T) graft provides an artificial systemic-to-pulmonary shunt as a palliative procedure for children and neonates with diminished pulmonary blood flow due to congenital heart disease (1–3). The procedure consists of the insertion of a polytetrafluoroethylene (PTFE, Gore-Tex) graft between a subclavian (or the innominate) artery and a pulmonary artery on the left or right side. The blockage of the shunt (stenosis or thrombosis), inadequate or excessive pulmonary blood flow,

asymmetric flow to the lungs, and stenosis or distortion of the pulmonary artery, are the potential complications of the procedure (1–3). With patient growth the flow through the graft with fixed cross-section can be limited and become insufficient (1–3). The control of the volume flow and the resistance of the vessels in this part of the circulatory blood system and the prediction of the hemodynamic conditions after surgery are in general difficult, although possible to some extent (2,3).

Computational fluid dynamic (CFD) methods have been applied to many problems related to blood flow in large vessels (4) with applications in cardiovascular surgery (5,6) and for artificial organ design (7). The problems from pediatric surgery included

Received April 2004; revised February 2005.

Address correspondence and reprint requests to Dr. Jacek Waniewski, Interdisciplinary Center of Mathematical and Computer Modelling, Warsaw University, Pawlowskiego 5a, PL 02–106 Warsaw, Poland. E-mail: jacekwan@icm.edu.pl

systemic-to-pulmonary shunts (8,9) and cavopulmonary connections (6). Numerical simulations of the modified Blalock-Taussig shunts, which connect a systemic (subclavian or innominate) artery and a pulmonary artery and have a pulsatile flow and high pressure gradient, are more difficult for numerical studies. Nevertheless, some aspects of the mB-T hemodynamics were investigated using computer simulations and an *in vitro* model (8,9). The pressure-flow relationship was described for the system that comprised the innominate artery with its bifurcation, the mB-T graft, and the right pulmonary artery, and had a plane of symmetry (8,9). Both pulsatile and steady state flows were investigated in four different arrangements of the mB-T graft, which differed in the diameter, curvature, and angle (8,9).

The diameter of the graft must be a trade-off between the vessel size, the danger of pulmonary edema if the flow through the graft is high, and insufficiency of the flow and clotting problems if the graft is too narrow. The risk associated with the modified Blalock-Taussig operation is low (1-3). The shunt patency was found to depend on the prosthesis diameter: the patency for 5 mm grafts was greater than for 4 mm ones (1). The common established cause of shunt failure was the occlusion of the graft at the graft-pulmonary artery anastomosis or in the pulmonary artery (1). Clotting of the graft occurs in spite of its perfectly antithrombotic surface. The more common occlusion of narrow compared to wide grafts suggests that the geometry of the graft and the flow pattern within it and in the vicinity of the entrance to and exit from it may contribute to the initiation and development of the thrombotic process. A possible relationship between the flow and clotting is through the shear-stress induced activation of platelets (10).

The effect of high shear stress on platelet activation, signaling system, aggregation, and adhesion to (damaged) endothelial wall is well established in experimental systems (10). Pathologically high levels of shear stress (e.g., in a stenosed coronary artery) are considered to be responsible for platelet thrombus formation (10). An artificial systemic-to-pulmonary shunt induces high flow due to the high pressure gradient in the vessels with rather unnatural geometry of anastomoses between the graft and the subclavian and pulmonary arteries. Although some flow-pressure characteristics of the graft were investigated (8,9), the geometry of the flow distribution and the details of flow characteristics are not known. The objective of the present study was to check, using computer fluid dynamics methods, whether high shear stress appears within the graft, and whether the

distribution of the flow in the graft and its vicinity can contribute to thrombus formation.

The shear stress was recently the subject of many CFD studies on fluid-vessel wall interactions using the wall shear stress (11-15) or the traction vector (16,17) as indicators of the strength of the interaction. The appearance of very low or very high wall shear stress/traction vectors and temporal oscillations of wall shear stress/traction vectors were investigated because of their impact on the neointimal thickening, endothelium growth, and stimulation of platelet aggregation (4). Low (<1 Pa) wall shear stress was related to intimal hyperplasia in arterio-arterial grafts and stented vessels (12,14,17,18), whereas high (>3.4 Pa) wall shear stress was related to intimal hyperplasia in the arterio-venous grafts (14). The region of flow stagnation in the end-to-side anastomosis with high pressure and high stress may also be a site of intimal hyperplasia and platelet deposition (4,14). In fact, the stenosis of the pulmonary artery at its anastomosis with the modified Blalock-Taussig graft is often reported (19,20). On the other hand, regions with low flow, e.g., stagnation or recirculation, were also identified as the sites of thrombotic depositions in other systems (21).

In the present study the activation of platelets inside the blood flow by high shear rate is the main subject of interest. Therefore, the volume of the system with shear rate over a threshold value is calculated as the main indicator of the conditions for platelet activation (22). Abnormally low and high wall shear stress is also investigated as the possible source of neointimal thickening and stenosis of arteries. Furthermore, the regions of flow stagnation or recirculation are identified.

METHODS

The 3D geometry of blood vessels was obtained from a CT scan in a child with a normal arrangement of the large vessels. The left subclavian artery (LSA) and the left (LPA) and right (RPA) pulmonary arteries were selected for the model (Fig. 1). The vessels were straightened and elongated at both sides to avoid possible entrance/exit artifacts during numerical simulations. Nevertheless, their relative position and some degree of curvature were left as in the original geometry (Fig. 1). The diameter of LSA was 4.5 mm and its length 40 mm, and the diameter of LPA and RPA was 7 mm and their joint length 45 mm. The mB-T graft was added to the model with five different shapes: two different diameters of 3 and 4 mm; two different curvatures for each shunt diameter (straight and curved, with lengths of 17.5 and

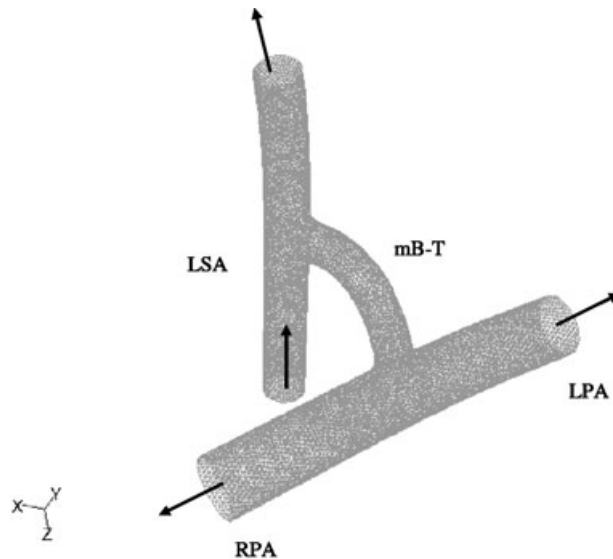


FIG. 1. The geometry of the model with the left subclavian artery (LSA), the left pulmonary artery (LPA), the right pulmonary artery (RPA), and the modified Blalock–Taussig graft (mB–T).

19 mm, respectively); and one narrowed, straight graft of 4 mm diameter at the anastomosis with LSA and 3 mm diameter at the anastomosis with LPA, and a length of 17.5 mm (Fig. 2). The angle between the graft and the blood vessel at the site of anastomosis was 90 degrees for all anastomoses. Note that there is no plane of symmetry for this system.

Tetrahedral mesh grids were created for the straight 3 mm model geometry with 120 000 and 150 000 cells. The mesh with 120 000 cells was found to provide a good convergence during the simula-

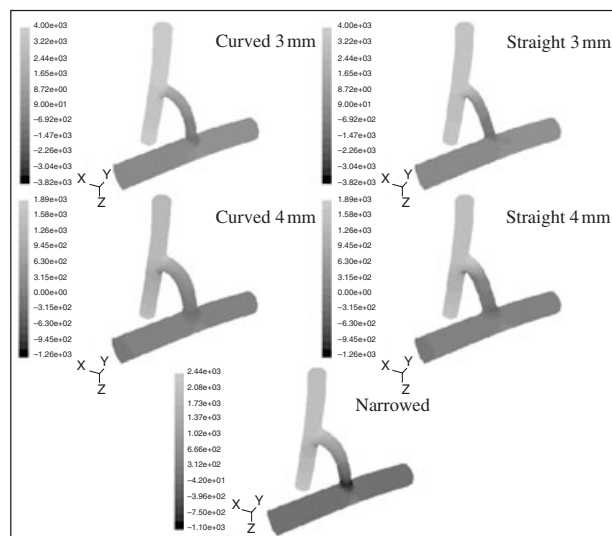


FIG. 2. The geometry of five different models of the mB–T graft. The distribution of hydrostatic pressure for the maximal flow obtained by numerical simulations is shown.

tions, with no further improvement for the larger mesh. Therefore, a grid with about 120 000 cells was used for each of the model geometries, with slight variation dependent on the size of the graft. The parameters of the grid quality were (for straight 4 mm graft): average cell volume $1.97 \times 10^{-5} \text{ cm}^3$ (range $0.25\text{--}5.93 \times 10^{-5} \text{ cm}^3$), average skewness 0.30 (range $1 \times 10^{-6}\text{--}0.75$), size change 1.32 (range 0.35–5.03), average edge ratio 1.52 (range 1.00–3.18), average aspect ratio 1.24 (range 1.00–3.37).

The Navier–Stokes and the continuity equations for incompressible fluid:

$$\rho \left(\frac{\partial v}{\partial t} + (v \cdot \nabla) v \right) = -\nabla p + \mu \Delta v$$

$$\nabla \cdot v = 0$$

where v is fluid velocity vector, p is fluid hydrostatic pressure, ρ is fluid density, and μ is fluid viscosity, were solved using the finite volume method and the Fluent 6 general-purpose computer code (Fluent Inc, Lebanon, NH, U.S.A.). The implicit, unsteady, laminar flow, second order solver was applied. In this study, blood was described as a Newtonian fluid with constant density 1060 kg/m^3 and viscosity 0.004 kg/(ms) . The wall was considered rigid, impermeable, and with a no-slip boundary condition.

The computer simulations were performed for time-dependent inflow velocities at the inlet to LSA with time-averaged volume inflow of 0.81 L/min , average velocity 0.86 m/s , and pulse rate 120 beats per minute (Fig. 3). The inflow pattern resembled that used in (8), and reflected the increased pulse rate and the increased left ventricle ejection volume in children with systemic-to-pulmonary shunts (23). The outlet boundary conditions were set to 0.4 of the mass inflow at each of the pulmonary arteries, and to 0.2 of the mass inflow at the outlet from the left subclavian artery. A similar distribution of blood flow (flow through the shunt of 70–80% of the inflow to

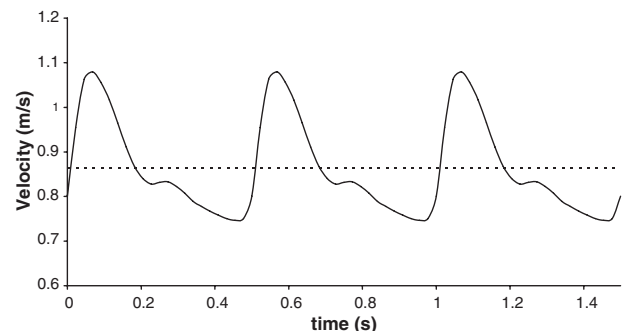


FIG. 3. The velocity at the inlet to the left subclavian artery vs. time (continuous line). Three heart beats are shown. Dashed line: the average velocity.

TABLE 1. Pressure drop between the inlet to the system (LSA In) and three outlets from the system: the left pulmonary artery (LPA Out), the right pulmonary artery (RPA Out), and the left subclavian artery (LSA Out), for the five different mB-T grafts and for the maximal (systole) and minimal (diastole) flow rate in the system

Graft	Pressure drop LSA in – LPA out (Pa)		Pressure drop LSA in – RPA out (Pa)		Pressure drop LSA in – LSA out (Pa)	
	Systole	Diastole	Systole	Diastole	Systole	Diastole
Straight 3 mm	3392	2060	3587	2146	211	175
Straight 4 mm	1571	954	1670	991	171	163
Curved 3 mm	3673	2264	3873	2359	207	179
Curved 4 mm	1432	914	1491	935	184	166
Narrowed	2142	1343	2220	1376	199	177

the system) was estimated for an in vivo shunt (9). The Reynolds numbers in the system were below 1900. The solver time step was 0.002 s. The convergence criterion was 10^{-7} .

In a postprocessing step, the fractional volume of the computational domain with shear-rate values higher than a threshold one was computed. Due to discretization, the shear rate may be assumed to be constant in each cell. Thus, all the computations were performed elementwise. The shear rate value was calculated based on derivatives of velocity components from the second invariant of the strain tensor (13). Volumes of cells with shear rate over the threshold value were summed up and finally divided by the total volume of the model (LSA, graft, LPA, and RPA). All the computations were performed in the Fluent environment with the use of a user-defined function (UDF). The threshold of pathologic shear rate was chosen as 2500 L/s, according to (10). The second threshold of a very high shear rate was selected as 7500 L/s; such high shear rate may appear in a stenosed coronary artery and is often associated with platelet thrombus formation (10).

RESULTS

The distribution of hydrostatic pressure in the system is shown in Fig. 2. Most of the pressure drop between the inlet and the outlet from the pulmonary arteries occurs in the initial part of the graft. The pressure drop along the graft is considerable for the 4 mm grafts (about 1500 Pa at the moment of the maximal inflow to the system (systole), and about 900–1000 Pa at the moment of the minimal inflow to the system (diastole) and increases by a factor of more than two for the 3 mm grafts (Table 1). However, the pressure drop along the graft is only about 50% higher for the narrowed graft than for the 4 mm grafts. The pressure drop between the inlet and the RPA outlet is slightly higher than the pressure drop to the LPA outlet (Table 1), because of the difference in the distance

from the graft anastomosis to the respective outlet from the pulmonary artery.

The flow patterns within all five models are rather complex. The streamlines demonstrate the vortices in LSA downstream from the bifurcation of the graft and in both pulmonary arteries, where the flow tends toward the screw geometry (Fig. 4). The qualitative flow pattern is similar for all five models (except for an eddy in the graft, see below). The magnitude of velocity in the longitudinal cross-section of the graft and LSA and in the transversal cross-section of LPA is shown in Fig. 5. The regions of low velocity are seen in LSA downstream from the bifurcation of the graft and in LPA. The channeling of the stream is also visible in LSA downstream from the bifurcation of

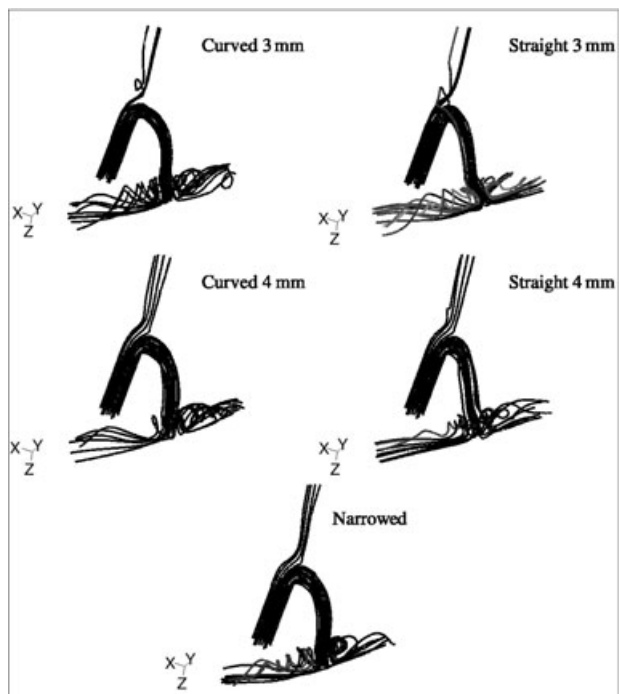


FIG. 4. Flow streamlines for the maximal flow in the five different models of the mB-T graft.

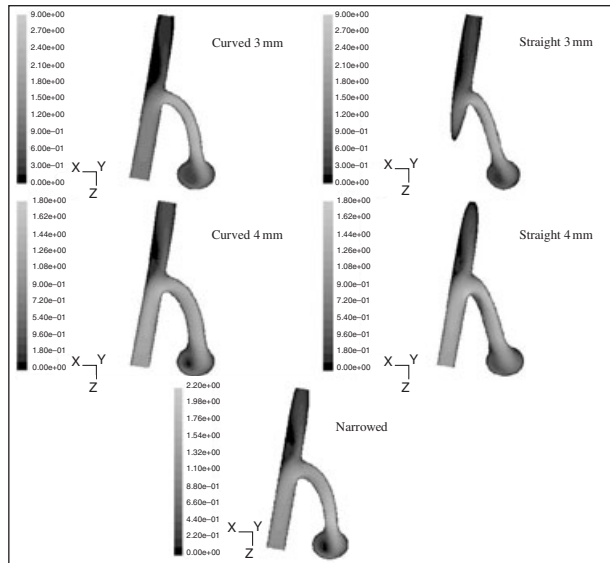


FIG. 5. The distribution of velocity magnitude for the maximal flow in longitudinal cross-sections of the five models of the mB-T graft.

the graft, and in LPA with a tendency to the screw flow. The area of low velocity was found also within the straight graft of 4 mm diameter, downstream from the inlet to the graft (Fig. 5). The velocity vectors demonstrate an eddy at this localization (Fig. 6), which is present during the whole cardiac cycle. No vortices within the graft were found in the other models.

The high shear rates were persistent in all five models during the whole cardiac cycle (Table 2 and Fig. 7). The highest values appeared in the 3 mm and the lowest in the 4 mm grafts (Table 2), mostly in a region close to the wall of the graft (Fig. 7). The maximal values of the shear rate were over 10 000 L/s during the whole cardiac cycle (Table 2). The fractional volume of the model occupied by high shear rate was between 2.6% and 4.5% if the threshold value of the shear rate was 2500 L/s, and between 0 and 1.4% if the threshold value was 7500 L/s (Table 2). The volume fraction was higher for the 3 mm than for the

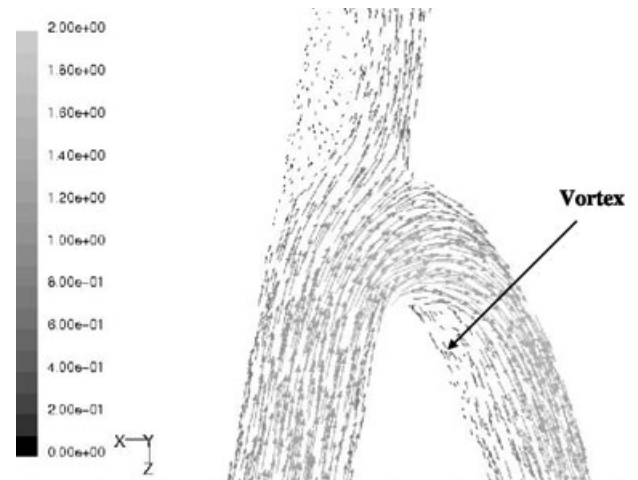


FIG. 6. The velocity vectors for the maximal flow in a longitudinal cross-section of the inlet to the straight 4 mm graft.

4 mm grafts, and higher for the curved than for the straight grafts. The shear rate in the narrowed graft was between the values for the 3 mm and 4 mm grafts. The values of the shear rate over 7500 L/s were persistent during the systole over a substantial part of the system only in the 3 mm grafts (Table 2). The high shear rate (>2500 L/s) was found in LSA upstream from its anastomosis with the graft, in the graft, and in the pulmonary artery close to its anastomosis with the graft, whereas the very high shear rate (>7500 L/s) was found exclusively in the graft (Fig. 7).

The low (<1 Pa) wall shear stress was found in the pulmonary arteries from the outlet of the graft toward their outlets, and in the downstream part of LSA, and it was persistent throughout the cardiac cycle (Fig. 8). In contrast, the high (>3.5 Pa) wall shear stress was identified in the upstream part of LSA, the graft, and in the pulmonary artery at the outlet from the graft (Fig. 8). The highest (over 40 Pa) wall shear stress appeared in the graft. In the vicinity of the anastomosis of the graft and LPA, the wall shear stress forms a sophisticated pattern with large surface gradients (Fig. 8).

TABLE 2. The fractional volume with the shear rate over two threshold values and the maximum shear rate at the maximal (systole) and at the minimal flow (diastole) in the five different models of the mB-T graft

Graft	Volume fraction with shear rate over 2500 1/s (%)		Volume fraction with shear rate over 7500 1/s (%)		Maximum shear rate (1/s)	
	Systole	Diastole	Systole	Diastole	Systole	Diastole
Straight 3 mm	4.0	3.0	1.2	0.7	27 023	18 024
Straight 4 mm	3.5	2.6	1.0	<0.1	23 189	15 272
Curved 3 mm	4.5	3.3	1.4	0.8	27 854	18 968
Curved 4 mm	3.6	2.7	1.0	<0.1	16 411	10 781
Narrowed	3.9	3.0	1.3	0.2	22 239	13 836

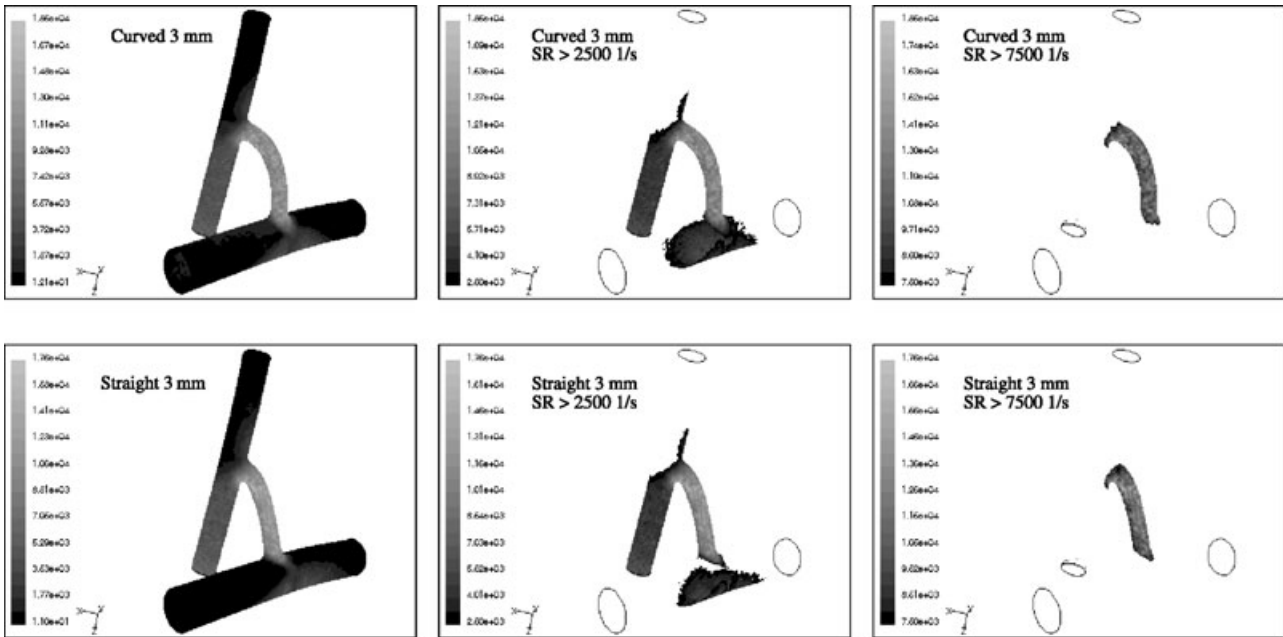


FIG. 7. Shear rate (SR, left panels), shear rate higher than 2500 L/s (middle panels), and shear rate higher than 7500 L/s (right panels) for the maximal flow at the wall of the vessels for models with 3 mm curved (upper panels) and straight (lower panels) grafts.

DISCUSSION

Virchow’s triad for the thrombus formation includes the composition of blood, the status of the internal surface of the blood vessels, and the blood flow (10,21). In the present study we investigated in

detail the flow pattern in the modified Blalock–Tausig graft of different geometries. Clotting, although not very common, is a leading cause of graft failure (1). Platelets can be activated by high shear stress and start the clotting process (10). Nevertheless, some other conditions must accompany the initiation of the

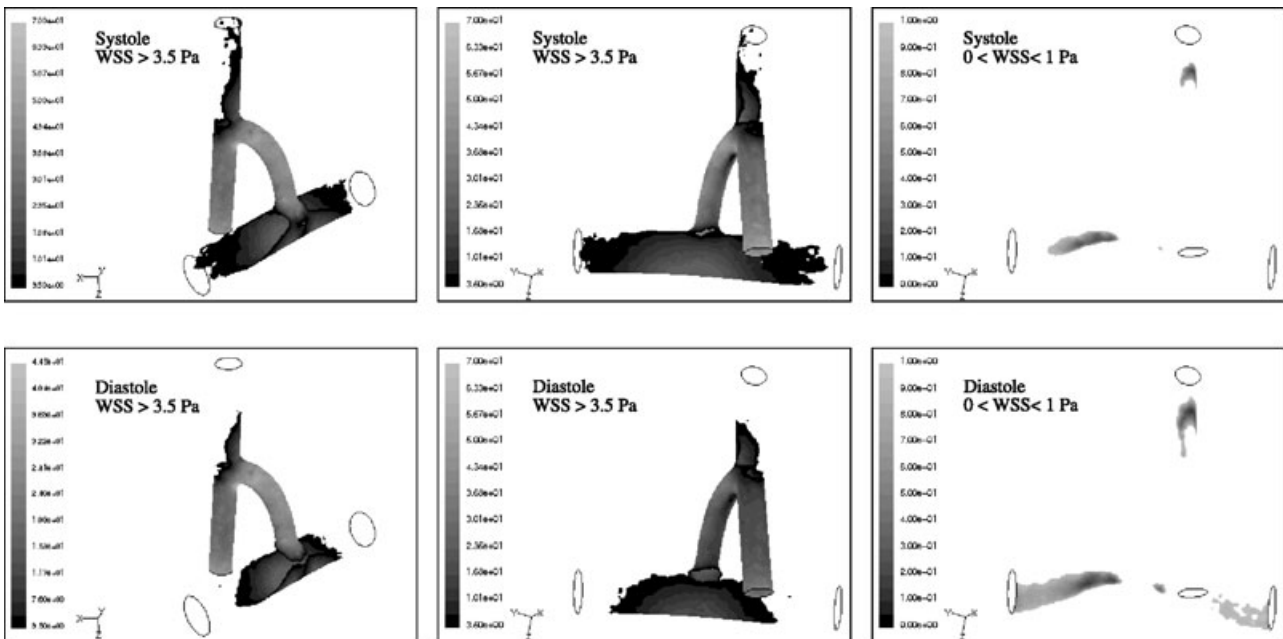


FIG. 8. Wall shear stress (WSS) over 3.5 Pa (left and middle panels for two different view angles) and less than 1 Pa (right panels) on the surface of the model with the 4 mm curved graft for the maximal flow (systole, upper panels) and minimal flow (diastole, lower panels).

thrombus formation. These may be, for example, the increased concentration of platelets, fibrinogen, von Willebrand factor, and/or other procoagulants; this is the first component of Virchow's triad – blood composition. The second component (vessel walls) may contribute to the thrombus formation if demasquation or other damage of the endothelium in the vicinity of the graft occurs, whereas the graft wall itself does not contribute to the clotting process.

A shear rate high enough to activate platelets (>2500 L/s), is present for the whole cardiac cycle in all five types of the graft geometry. The 3 mm grafts have a higher fractional volume with high shear rate than the 4 mm grafts, and therefore higher probability of platelet activation. On the other hand, the platelet activation depends not only on the strength of shear stress but also on the time the platelet is subjected to this stress (10). The velocity of blood in thin grafts is, in general, higher than in large diameter grafts if the volume flow is the same in both types of grafts, and therefore platelets pass small diameter grafts faster than larger diameter ones. Both factors, high shear rate and time of its effect on platelets, act in the opposite direction, and may cancel each other to some extent. More detailed quantitative knowledge of these phenomena is still lacking.

The difference between grafts with different diameters and shapes is more pronounced in the case of very high shear rates (>7500 L/s). Although the fractional volume showing very high shear rate is similar ($\geq 1\%$) in all five types of the graft during the systole, very high shear rate is present during the diastole mainly in the 3 mm grafts (Table 2). The blood velocity is lower during the diastole, and the time platelets spend under this very high shear rate is longer. Therefore, the probability of platelet activation is higher in the 3 mm grafts. Very high shear rates are empirically associated with platelet type thrombus in stenosed coronary arteries (10). One may hypothesize that the very high shear rate persistent throughout the whole cardiac cycle in the 3 mm grafts may be responsible, in the presence of additional prothrombotic factors, for the thrombus formation in or downstream from the graft.

The fractional volumes of the very high shear rate (>7500 L/s) were not higher than 1–1.4%. They were however, calculated against the volume of the whole system. The graft volume, where this very high shear rate appeared exclusively (Fig. 7), is between 5% and 9% of the whole system volume, depending on the diameter and the length of the graft. Therefore, one may infer that the very high shear rate prevailed in c. 10–25% of the graft volume during the systole. Furthermore, although the high shear rate (>2500 L/s)

prevailed not only in the graft but also upstream and downstream from it (i.e., in about 50% of the whole system volume), they were concentrated mostly in the graft. The percentage of platelets that may be affected by such a high or very high shear rate may therefore be estimated roughly as 20–40% of all platelets that flow through the graft.

The diameter of the graft determines the high shear rate fractional volume more strongly than the shape of the graft, at least among the shapes investigated in the present study (Table 2). The pressure drop along the graft is also determined mainly by the graft's diameter (Table 1). The last observation is in agreement with the results of the investigations of the pressure–flow relationship in the mB–T grafts (8). The pressure drop found in the present study is similar to those described in (8). The graft diameter is generally recognized as the main regulator of the flow in systemic-to-pulmonary shunts (1–3).

The computer simulations in the present study were performed for the same volume flow through the graft, and this resulted in different pressure drops for different grafts. The hydrostatic pressure in the systemic and pulmonary circulations *in vivo* may be regulated, to some extent, independently from each other and from the graft diameter. Such independent changes may result in turn in various volume flows and flow patterns in the graft and its upstream and downstream connections. Thus, the conditions for the stimulation of platelets may vary for the same geometry of graft. This variability must also be taken into account when discussing the clotting of the mB–T grafts. Our study provides only some insight into the problem by demonstrating the possible link of the increased shear rate in the graft and the probability of thrombus formation.

The hypothetical process of clotting may be described as follows. Platelets, stimulated by a very high shear rate within the graft, aggregate in the eddy regions with low fluid velocity that exist close to the outlet of the graft to the pulmonary artery. The aggregation may be also possible within the graft if an eddy forms downstream from the inlet to the graft. The main factor that may contribute to graft clotting is the small diameter of the graft, in agreement with clinical observations (1–3). Clotting is not common, so some additional factors are necessary, such as change in blood composition, changes in the endothelium of the pulmonary artery wall, or abnormal flow magnitude or pattern.

The appearance of abnormal wall shear stress at the vessel wall upstream and downstream from the graft (Fig. 8) may decrease the antithrombotic activity of endothelial cells, which under physiological

conditions release various vasoactive and antithrombotic agents (10,17,18). The balance of all the factors that stimulate or prevent thrombus formation in the system with mB-T graft is difficult for a quantitative analysis, and some additional, contingent (compared to the flow pattern) factors may also contribute to the shift of balance toward the initiation of the thrombus formation.

The high (>3.5 Pa) and highly spatially variable wall shear stress at the graft-to-pulmonary artery anastomosis may induce neointimal thickening or damage to the endothelium (14). In some patients the inflow from the pulmonary trunk (not taken into account in our simulations), although reduced below its normal rate, may change the flow and shear stress in the pulmonary artery. Nevertheless, the abnormal wall shear rate in both arteries connected by the Blalock-Taussig graft can contribute to some changes of the vessel wall, which may in turn contribute to the change in the flow through the graft. The site of anastomosis of the graft and pulmonary artery seems to be especially prone to the formation of stenosis because of the abnormal pattern of wall shear stress found in our simulations. Clinical observations are in agreement with this finding (19,20). The relatively frequent formation of stenosis at this site was attributed to the surgical procedure itself, the distortion (tenting) of the pulmonary artery, and/or to the flow conditions at the site (20). The first two factors can be important, but the finding of the stenoses in the pulmonary arteries in patients with the patent ductus arteriosus (with no surgery and generally no distortion of the pulmonary artery at the site of ductus-to-pulmonary artery anastomosis (20)) shows that the flow conditions are also among important contributors to the stenosis formation at the systemic-to-pulmonary shunts. Note that the complex flow pattern at this anastomosis depends, at least in part, on the deviation of the connection between the graft and the artery from the longitudinal centerline of the artery, which results in the asymmetric channeling of the flow along the artery wall easily seen in the cross-section of the pulmonary artery (Fig. 5). A similar complex flow pattern at the entrance to and exit from the graft, with eddies in the pulmonary artery, was found by laser visualization in a physical model of mB-T (24).

The eddy in the subclavian artery downstream from the anastomosis of the graft may also be a site of thrombus formation, which may start if the clotting cascade is initiated by other factors in the body than the flow pattern in the graft. The eddies like those demonstrated in the present study rarely occur in the vascular system, and are the result of abnormal

bifurcations at the upstream and downstream anastomoses of the graft with the subclavian and pulmonary artery, respectively. This abnormality, together with a fast flow through the graft created by the high pressure difference between the systemic and pulmonary circulations, may be considered as the cause for the unusual flow pattern that may promote clotting of the graft and/or pulmonary artery.

The narrowed graft (funnel) is an example of possible modifications of the graft shape that, although not applied currently, can be considered as a candidate for optimized shunt geometry. The desirable characteristics of the flow through the graft, such as the pressure-flow relationship, shear rate, wall shear stress, etc., which can be formulated to provide the required flow rate and decrease the probability of thrombus and/or stenosis formation, may be optimized in terms of size and shape of the graft by looking at the real anatomy of patient vessels and computer simulations.

CONCLUSION

We conclude that computer simulations revealed a complex flow pattern within the modified Blalock-Taussig graft and its upstream and downstream arteries with pathological values of shear stress, eddies, and spiral flow. This pattern may contribute to the processes of thrombosis and stenosis that are frequent complications of this therapy. Small diameter grafts yield more severe deviations from the normal physiological conditions and may be more prone to clot. This finding is in agreement with clinical observations. More detailed investigations of thrombosis and stenosis in systemic-to-pulmonary shunts need more biological information about the processes and better separation of flow-induced complications from those caused by other reasons.

Acknowledgment: This study was supported by a grant from the Polish Committee of Scientific Research, Project no. 7T11F01820.

REFERENCES

1. de Leval MR, McKay R, Jones M, Stark J, Macartney FJ. Modified Blalock-Taussig shunt. Use of subclavian artery orifice as flow regulator in prosthetic systemic-pulmonary artery shunts. *J Thorac Cardiovasc Surg* 1981;81:112-9.
2. de Leval MR. Systemic-to-pulmonary artery shunts. In: Stark J, de Leval MR, eds. *Surgery for Congenital Heart Defects*. Philadelphia, PA: Saunders, 1997;247-57.
3. Doty DB. Palliative operations. In: Arciniegas E, ed. *Pediatric Cardiac Surgery*. Chicago, IL: Year Book Medical Publishers 1985, 57-66.
4. Quarteroni A, Tuveri M, Veneziani A. Computational vascular dynamics: problems, models and methods. *Comput Visual Sci* 2000;2:163-97.

5. Cape EG. Mathematical modeling in the evaluation and design of surgical procedures. *J Thorac Cardiovasc Surg* 1996; 111:499–501.
6. de Leval MR, Dubini G, Migliavacca F, et al. Use of computational fluid dynamics in the design of surgical procedures: application to the study of competitive flows in cavo-pulmonary connections. *J Thorac Cardiovasc Surg* 1996;111:502–13.
7. Verdonck P. The role of computational fluid dynamics for artificial organ design. *Artif Organs* 2002;26:569–70.
8. Migliavacca F, Dubini G, Pennati G, et al. Computational model of the fluid dynamics in systemic-to-pulmonary shunts. *J Biomech* 2000;33:549–57.
9. Pennati G, Fiore GB, Migliavacca F, Lagana K, Fumero R, Dubini G. In vitro steady-flow analysis of systemic-to-pulmonary shunt haemodynamics. *J Biomech* 2001;34:23–30.
10. Kröll MH, Hellums JD, McIntire LV, Schafer AI, Moake JL. Platelets and shear stress. *Blood* 1996;88:1525–41.
11. Shu MC, Hwang NH. Haemodynamics of angioaccess venous anastomoses. *J Biomed Eng* 1991;13:103–12.
12. Goubergrits L, Affeld K, Wellnhöfer E, Zurbrugg R, Holmer T. Estimation of wall shear stress in bypass grafts with computational fluid dynamics method. *Int J Artif Organs* 2001;24:145–51.
13. LaDisa JF Jr, Guler I, Olson LE, et al. Three-dimensional computational fluid dynamics modeling of alterations in coronary wall shear stress produced by stent implantation. *Ann Biomed Eng* 2003;31:972–80.
14. Krueger U, Zanow J, Scholz H. Computational fluid dynamics and vascular access. *Artif Organs* 2002;26:571–5.
15. Frank AO, Walsh PW, Moore JE Jr. Computational fluid dynamics and stent design. *Artif Organs* 2002;26:614–21.
16. Taylor CA, Hughes TJ, Zarins CK. Finite element modeling of three-dimensional pulsatile flow in the abdominal aorta: relevance to atherosclerosis. *Ann Biomed Eng* 1998;26:975–87.
17. Younis HF, Kaazempur-Mofrad MR, Chung C, Chan RC, Kamm RD. Computational analysis of the effects of exercise on hemodynamics in the carotid bifurcation. *Ann Biomed Eng* 2003;31:995–1006.
18. Benard N, Coisne D, Donal E, Perrault R. Experimental study of laminar blood flow through an artery treated by a stent implantation: characterisation of intra-stent wall shear stress. *J Biomech* 2003;36:991–8.
19. Godart F, Qureshi SA, Simha A, et al. Effects of modified and classic Blalock-Taussig shunts on the pulmonary arterial tree. *Ann Thorac Surg* 1998;66:512–7.
20. Sachweh J, Dabritz S, Didilis V, Vazquez-Jimenez JF, v Bernuth G, Messmer BJ. Pulmonary artery stenosis after systemic-to-pulmonary shunt operations. *Eur J Cardiothorac Surg* 1998;14:229–34.
21. Gartner MJ, Wilhelm CR, Gage KL, Fabrizio MC, Wagner WR. Modeling flow effects on thrombotic deposition in a membrane oxygenator. *Artif Organs* 2000;24:29–36.
22. Mizerski J, Waniewski J, Trykozko A. Thrombotic complications of modified Blalock-Taussig (MBT) anastomosis: a computer study. Paper presented at XXXVIII Congress of the European Society for Surgical Research, 2003, Ghent, Belgium. Available at: <http://www.essr2003.be>. Accessed 2003.
23. Guyton AC. *Human Physiology and Mechanisms of Disease*. New York, NY: Saunders, 1987.
24. Malota Z, Nawrat Z, Kostka P, Mizerski J, Nowinski K, Waniewski J. Physical and computer modelling of blood flow in a systemic-to-pulmonary shunt. *Int J Artif Organs* 2004;27: 990–9.